

Superluminal propagation of pulsed pseudo-thermal light in atomic vapor

In-Ho Bae,¹ Young-Wook Cho,² Hee Jung Lee,¹ Yoon-Ho Kim,^{2,3} and Han Seb Moon^{1,4}

¹*Department of Physics, Pusan National University, Busan, 609-735, Korea*

²*Department of Physics, Pohang University of Science and Technology (POSTECH), Pohang, 790-784, Korea*

³*yoanho72@gmail.com*

⁴*hsmoon@pusan.ac.kr*

Abstract: We report an experimental demonstration of slow and superluminal propagation of pseudo-thermal (chaotic) light in the Λ -type system of the $5S_{1/2}$ - $5P_{1/2}$ transition of ^{87}Rb atom. The slowed propagation of pulsed pseudo-thermal light was demonstrated in an electromagnetically-induced transparency medium while the superluminal propagation was demonstrated with the enhanced absorption scheme where the coupling field takes the form of a standing wave. We have also demonstrated that the photon number statistics of the pseudo-thermal light is preserved for both the subluminal and superluminal cases.

© 2010 Optical Society of America

OCIS codes: (270.5290) Photon statistics; (270.5290) Coherent optical effects.

References and links

1. L. V. Hau, S. E. Harris, Z. Dutton, and C. H. Behroozi, "Light speed reduction to 17 metres per second in an ultracold atomic gas," *Nature* **397**, 594–597 (1999).
2. M. M. Kash, V. A. Sautenkov, A. S. Zibrov, L. Holberg, G. R. Welch, M. D. Lukin, Y. Rostovtsev, E. S. Fry, and M. O. Scully, "Ultraslow Group Velocity and Enhanced Nonlinear Optical Effects in a Coherently Driven Hot Atomic Gas," *Phys. Rev. Lett.* **82**, 5229–5232 (1999).
3. K. Kim, H. S. Moon, C. Lee, S. K. Kim, and J. B. Kim, "Observation of arbitrary group velocities of light from superluminal to subluminal on a single atomic transition line," *Phys. Rev. A* **68**, 013810 (2003).
4. H. Kang, G. Hernandez, and Y. Zhu, "Superluminal and slow light propagation in cold atoms," *Phys. Rev. A* **70**, 011801 (2004).
5. D. F. Phillips, A. Fleischhauer, A. Mair, R. L. Walsworth, and M. D. Lukin, "Storage of Light in Atomic Vapor," *Phys. Rev. Lett.* **86**, 783–786 (2001).
6. S. E. Harris, "Electromagnetically induced transparency," *Phys. Today* **50**, 36–42 (1997).
7. Y.-W. Cho and Y.-H. Kim, "Storage and Retrieval of Thermal Light in Warm Atomic Vapor," eprint arXiv:0910.0074 (2009).
8. S. Chu, and S. Wong, "Linear pulse propagation in an absorbing medium," *Phys. Rev. Lett.* **48**, 738–741 (1982).
9. A. M. Steinberg, P. G. Kwiat, and R. Y. Chiao, "Measurement of the single-photon tunneling time," *Phys. Rev. Lett.* **71**, 708–711 (1993).
10. L. J. Wang, A. Kuzmich, and A. Dogariu, "Gain-assisted superluminal light propagation," *Nature* **406**, 277–279 (2000).
11. M. D. Stenner, D. J. Gauthier, and M. A. Neifeld, "The speed of information in a 'fast-light' optical medium," *Nature* **425**, 695–698 (2003).
12. R. W. Boyd and P. Narum, "Slow- and fast-light : fundamental limitations," *J. Mod. Opt.* **54**, 2403–2411 (2007).
13. I. H. Bae, H. S. Moon, M. K. Kim, L. Lim, and J. B. Kim, "Transformation of electromagnetically induced transparency into enhanced absorption with a standing-wave coupling field in an Rb vapor cell," *Opt. Express* **18**, 1389–1397 (2010).
14. H. S. Moon, S. E. Park, Y.-H. Park, L. Lim, and J. B. Kim, "Passive atomic frequency standard based on coherent population trapping in ^{87}Rb using injection-locked lasers," *J. Opt. Soc. Am. B* **23**, 2393–2397 (2006).

15. F. T. Arecchi, "Measurement of the Statistical Distribution of Gaussian and Laser Sources," *Phys. Rev. Lett.* **15**, 912–916 (1965).
 16. R. Hanbury-Brown and R. Q. Twiss, "Correlation between Photons in two Coherent Beams of Light," *Nature*, **177**, 27–29 (1956).
 17. M. Harris, G. N. Pearson, C. A. Hill, and J. M. Vaughan, "The fractal character of Gaussian-Lorentzian light," *Opt. Commun.* **116** 15–19 (1995).
 18. L. Mandel, "Fluctuations of Photon Beams: The Distribution of the Photo-Electrons," *Proc. Phys. Soc. (London)* **74**, 233 (1959).
 19. R. Loudon, "The Quantum Theory of Light," *The Quantum Theory of Light* (Oxford University Press) (2000).
-

1. Introduction

Coherent interaction between light and atomic system can alter the optical properties of a medium such as absorption and dispersion. Manipulating the dispersive property of a medium makes it possible to realize the control of light speed [1–5]. For example, a steep normal dispersive medium exhibits the ultra slow group velocity (slow light). Slow light has been attractive issues due to the possibilities of optical buffers and optical quantum memory. Based on the electromagnetically induced transparency (EIT), a two-photon atomic coherence effect, ultra-slow propagation of light pulse has been reported both in cold atom and in warm atomic vapor systems [1, 2, 6]. Recently, preservation of photon number statistics of thermal light in subluminal and light-storage experiments have been reported in Ref. [7].

On the other hand, the group velocity in an anomalous dispersive medium can exceed the vacuum speed of light c . Superluminal light propagation with a laser pulse has been demonstrated using anomalous dispersion in various systems [8–10]. Although the superluminal group velocity appears to be at odds with causality, it has been shown that information velocity does not exceed c [11]. Note also that, there exists a fundamental limit for fast light [12].

So far, the experimental realization of superluminal light has been done only with a coherent laser pulse. In this paper, we report an experimental demonstration of subluminal and superluminal propagation of pulsed (chaotic) thermal light in a hot Rb atomic vapor cell. Both slow and superluminal propagation are achieved in a single system. The slowed propagation of pulsed thermal light was demonstrated in an EIT medium. The superluminal propagation was demonstrated with the enhanced absorption (EA) scheme in which an additional counter-propagating coupling field to the EIT setting forms the standing wave coupling field [13]. We note that the EA scheme based on the standing-wave coupling field allows us to switch from the slow light condition to the superluminal condition for the pulsed pseudo-thermal probe in a single experimental setup. In addition, by measuring the photon count distribution, we demonstrate experimentally that the photon number statistics is preserved for the superluminal pulsed thermal light.

2. Experimental setup

The experimental schematic is shown in Fig. 1. Figure 1(a) shows the Λ -type atomic energy diagram of the D1-line of ^{87}Rb atom used for the experiment. When the strong co-propagating coupling field in a resonance with $F = 2 \rightarrow F' = 2$ transition is applied to the atomic ensemble, it becomes transparent to the weak probe field which is in a resonance with $F = 1 \rightarrow F' = 2$. The EIT medium exhibits the steep normal dispersion resulting in the slow light [6]. However, if the coupling field is made into a standing wave by adding an additional counter-propagating coupling field, the atomic ensemble now exhibits enhanced absorption (EA) [13]. We make use of the anomalous dispersion associated with the EA effect for demonstrating superluminal pulse propagation for the thermal light.

The experimental schematic is shown in Fig. 1(b). First, two diode lasers (one for the coupling and the other for the probe) with the frequency shift of 6.843 GHz are phase-locked by the

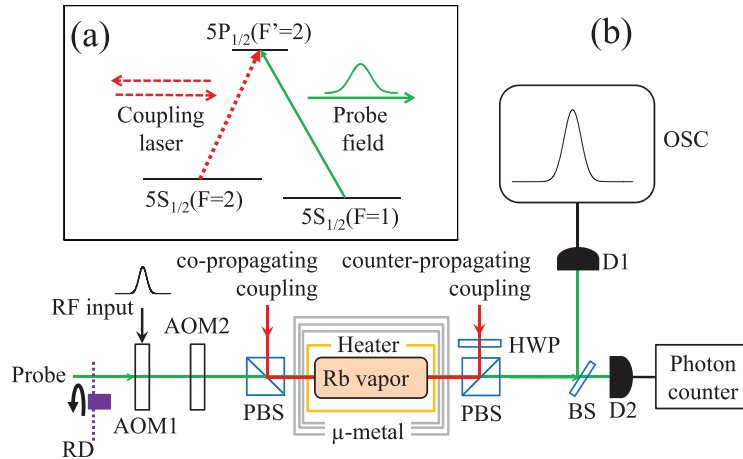


Fig. 1. (Color online) (a) $5S_{1/2}$ - $5P_{1/2}$ transition of ^{87}Rb atom is used as the Λ -type atomic system. (b) Schematic diagram of the experiment. Pseudo-thermal light is generated by focusing the probe laser on the rotating disk (RD). AOM1 is then used to make a pseudo-thermal light pulse. AOM2 is used for compensating the frequency shift due to AOM1. (BS: beam splitter, D1: Photo-current detector, D2: Single-photon counting detector, HWP: half-wave plate, PBS: polarization beam splitter, AOM: acousto-optic modulator).

optical injection locking technique [14]. The probe pulse was generated by the acousto-optic modulator (AOM1). An additional acousto-optic modulator (AOM2) is used to compensate the frequency shift due to AOM1. A rotating ground disk (RD) is inserted to generate the chaotic pseudo-thermal probe beam [7, 15]. The probe beam is then combined with the co-propagating coupling beam at the polarizing beam splitter (PBS). We use a 2.5 cm diameter and 5 cm long Rb vapor cell without buffer gas. To prevent Earth's magnetic fields, the vapor cell is wrapped with three layers of μ -metal sheets. The temperature of vapor cell is controlled with a thermal heater located inside of μ -metal shielding. In order to set the standing-wave condition of coupling field, the counter-propagating coupling beam is directed backward at the second polarizing beam splitter. The intensity of counter-propagating coupling beam is controlled with a half-wave plate (HWP). The probe field, after propagating through the vapor cell, is split into two by BS: one is used to measure the transmission spectrum with the photo-current detector D1 and the oscilloscope (OSC) and the other is used for photon number statistics measurement with the single-photon counting detector D2.

3. EIT and EA spectra

Let us first discuss the transmission spectra of the probe field. In Fig. 2(a), we show the transmission spectra of the laser probe measured by scanning the probe frequency while keeping the coupling laser frequency fixed. The power of laser probe was $10 \mu\text{W}$ and the power of co-propagating coupling beam was 3 mW. The temperature of the vapor cell was kept at 90°C . When only the co-propagating coupling beam is applied, the typical EIT spectrum is exhibited with the linewidth of 1.5 MHz. We then applied the counter-propagating coupling beam of the same power as the co-propagating coupling beam to form the standing-wave condition for the coupling field. Once the coupling field takes the form of a standing wave, the EIT effect disappears and the atomic ensemble now exhibits enhanced absorption (EA) [13]. The linewidth of EA is measured to be 3 MHz. The broadening of the EA spectrum is due to (i) the saturation effect of probe absorption from highly dense atomic medium and (ii) increased power of the

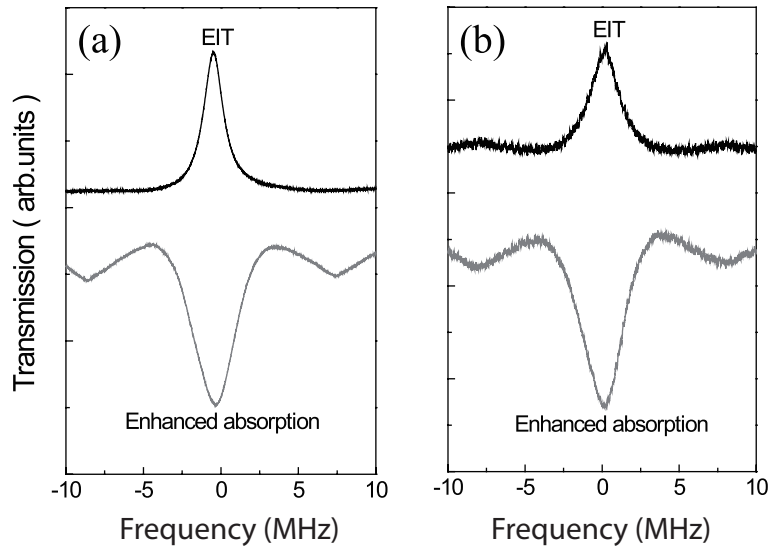


Fig. 2. The measured EIT and EA transmission spectra for the laser probe, (a), and the thermal light probe, (b), as a function of probe frequency. For the EIT spectra, a single co-propagating coupling laser is used and for the EA effect, an additional counter-propagating coupling laser forms the standing-wave coupling field. For laser probe, (a), the linewidths of EIT and EA are measured to be 1.5 MHz and 3 MHz, respectively. For thermal light probe, (b), they are 2 MHz and 3 MHz, respectively.

coupling field (i.e., an additional counter-propagating coupling field is present).

The transmission spectra for the thermal probe is shown in Fig. 2(b). For this measurement, the rotating ground disk is inserted into the path of the probe beam. The focused probe laser scattered from the rotating ground disk is known to exhibit thermal light characteristics and is used in this work as the thermal probe field [7]. The characteristics of the thermal probe were measured with a Hanbury-Brown-Twiss interferometry and the coherence time of the thermal probe was approximately $2 \mu\text{s}$, which corresponds to the spectral linewidth of 500 kHz [16]. The power of the thermal probe was measured to be $20 \mu\text{W}$. With the thermal probe beam, the linewidths of EIT and EA were measured to be approximately 2 MHz and 3 MHz, respectively, as shown in Fig. 2(b). The broadening of the EIT linewidth for the thermal probe, compared to the laser probe, is due to the broadened spectral linewidth of the thermal probe beam [17]. However, the EA spectrum for the thermal probe is identical to that of the laser probe, i.e., no broadening is observed for the EA spectrum, because of the saturation effect of probe absorption.

4. Pulse propagation

Let us now discuss the subluminal/superluminal propagation of thermal and laser probes. In all cases, the Gaussian-shaped probe pulse had the full-width at half maximum (FWHM) of 500 ns and was generated by AOM1 in Fig. 1. In Fig. 3(a), the experimental data for superluminal/subluminal pulse propagation for the laser probe are presented. The subluminal pulse propagation was demonstrated in the EIT condition and the superluminal pulse propagation was demonstrated in the EA condition [13].

In Fig. 3(b), the results for the thermal probe are shown. As before, thermal light was generated by scattering the probe laser off at the rotating ground disk and AOM1 is used to shape the

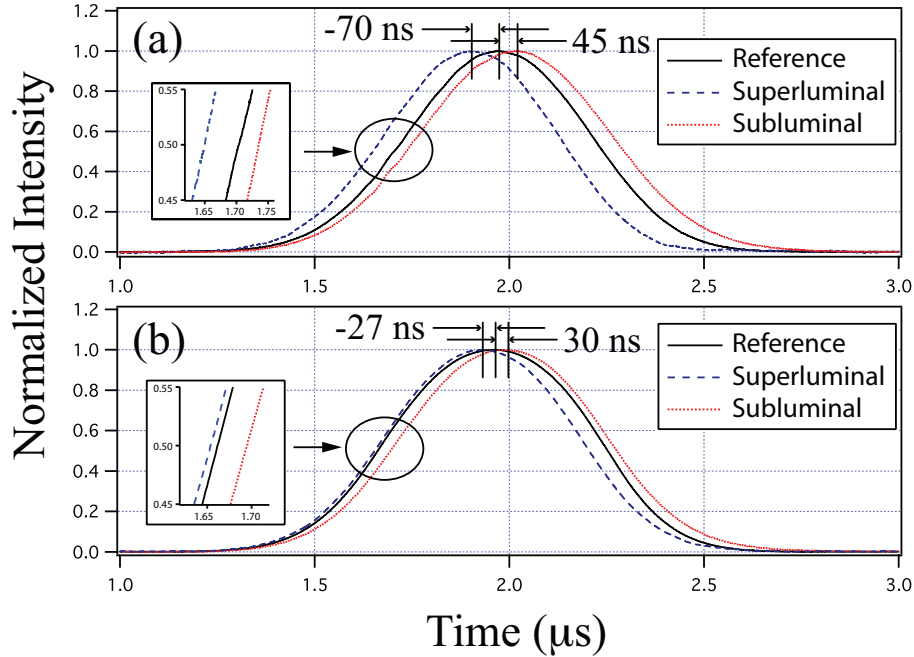


Fig. 3. (Color online) The superluminal and subluminal pulses generated from (a) the laser probe and from (b) the thermal probe. The reference pulse is measured with the coupling field turned off. For the laser probe, (a), the superluminal and subluminal pulses are, respectively, 70 ± 0.06 ns advanced and 45 ± 0.03 ns delayed with respect to the reference pulse. For the thermal probe, (b), superluminal and subluminal pulses are, respectively, a 27 ± 0.08 ns advanced and a 30 ± 0.09 ns delayed with respect to the reference pulse. The advance and delay times are measured by comparing the peak positions of the pulses.

thermal light into a Gaussian pulse. Although the amount of advance/delay of the peak positions of the thermal probe are slightly smaller with respect to the case of laser probe in Fig. 3(a), it is clear that the thermal probe exhibits superluminal and subluminal pulse propagation in the EA and EIT conditions, respectively.

5. Photon number statistics

We now explore experimentally if the photon number statistics of thermal light will be maintained in the superluminal pulse propagation of the EA scheme. It is well known that the laser beam (i.e., the coherent state) follows the Poisson photon number statistics given as [18, 19]

$$P_{coh}(n) = \frac{\bar{n}^n}{n!} \exp[-\bar{n}], \quad (1)$$

where \bar{n} is the average number of photons for a given measurement time. For thermal light, the corresponding photon number distribution is the Bose-Einstein distribution [18, 19],

$$P_{th}(n) = \frac{\bar{n}^n}{(1 + \bar{n})^{1+n}}. \quad (2)$$

In Fig. 3, we have demonstrated superluminal pulse propagation of thermal probe in the EA medium. It would therefore be interesting to investigate if the photon number statistics is maintained during the superluminal pulse propagation process through the EA medium.

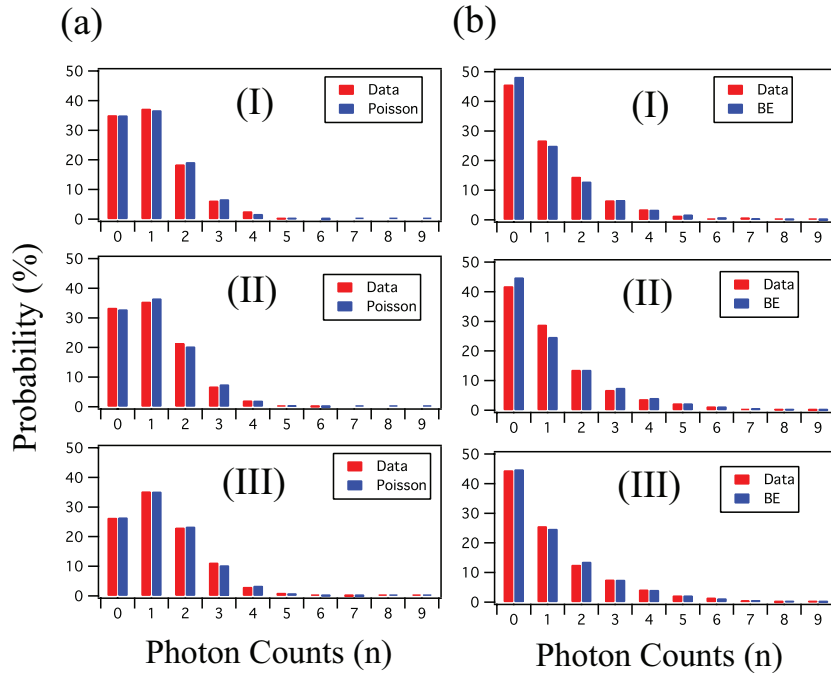


Fig. 4. (Color online) Photon number statistics in the cases of (I) superluminal pulse propagation in the enhanced absorption condition, (II) ordinary pulse propagation in the linear absorption regime with the coupling field turned off, and (III) subluminal pulse propagation in the EIT condition. The left column, (a), shows the results for the laser probe pulse and the right column, (b), shows the result for the thermal probe pulse.

In experiment, we have measured the photon counting events directly, by using the single mode fiber coupled single photon counting detector D2, for the optical pulse (laser and thermal) after passing the atomic medium. The measurement time was set at 800 ns which is shorter than the full coherence time of the optical pulse. Note that the measurement time window should be smaller than the coherence time of the optical pulse to faithfully measure the photon-number distribution of the pulse, see Ref. [7].

We obtain the photon number distribution for the laser probe and the thermal probe. The experimental results are shown in Fig. 4. The data show clearly that the laser probe pulse exhibits Poissonian photon-count distribution and the thermal probe pulse exhibits Bose-Einstein photon-count distribution in all three cases, namely, (I) superluminal pulse propagation in the enhanced absorption condition, (II) ordinary pulse propagation in the linear absorption regime with the coupling field turned off, and (III) subluminal pulse propagation in the EIT condition. The data in Fig. 4 can be used to evaluate the normalized second-order correlation coefficient $g^{(2)}$ [7, 19]

$$g^{(2)} = 1 + ((\Delta n)^2 - \bar{n}) / \bar{n}^2, \quad (3)$$

since $(\Delta n)^2 = \langle n^2 \rangle - \langle n \rangle^2$ and the average photon number \bar{n} can be calculated from the experimental data. Note that the probe field is attenuated by adjusting the single-mode fiber which is coupled to the (non-photon-number resolving) single-photon detector so that \bar{n} is kept approximately 1, see Ref. [7]. For the laser probe pulse, the calculated $g^{(2)}$ are 1.07 ± 0.08 , 1.06 ± 0.08 , and 1.01 ± 0.03 for the superluminal, the subluminal, and the ordinary pulse propagation conditions, respectively. For the thermal probe pulse, the calculated $g^{(2)}$ are 1.95 ± 0.15 , $1.87 \pm$

0.06, and 1.91 ± 0.09 for the superluminal, the subluminal, and the ordinary pulse propagation conditions, respectively. These values are in good agreement with the ideal values: $g^{(2)} = 1$ for coherent light and $g^{(2)} = 2$ for thermal light.

6. Summary

In summary, we have reported the subluminal and superluminal pulse propagation of thermal light in a hot Rb vapor cell by making use of the EIT and the EA conditions in a single system. We have also measured the photon count distribution and found that the photon number statistics is well preserved for the thermal probe pulse propagating through the atomic medium in the subluminal and superluminal pulse propagation conditions. These results suggest that it should be possible to control the speed of the probe pulse from subluminal to superluminal continuously while maintaining the statistical properties of the light pulse.

Acknowledgement

This work was supported by the National Research Foundation of Korea (2009-0070668, 2009-0073051, and 2009-0084473).